UC San Diego
UC San Diego Previously Published Works

Title

Phenotypic switching of adipose tissue macrophages with obesity is generated by spatiotemporal differences in macrophage subtypes.

Permalink

https://escholarship.org/uc/item/6w74w20b

Journal

Diabetes, 57(12)

ISSN

0012-1797

Authors

Lumeng, Carey N
DelProposto, Jennifer B
Westcott, Daniel J
et al.

Publication Date

2008-12-01

DOI

10.2337/db08-0872

Peer reviewed

Phenotypic Switching of Adipose Tissue Macrophages With Obesity Is Generated by Spatiotemporal Differences in Macrophage Subtypes

Carey N. Lumeng,[1,2,3] Jennifer B. DelProposto,[1] Daniel J. Westcott,[1] and Alan R. Saltiel[1,3,4]

OBJECTIVE—To establish the mechanism of the phenotypic switch of adipose tissue macrophages (ATMs) from an alternatively activated (M2a) to a classically activated (M1) phenotype with obesity.

RESEARCH DESIGN AND METHODS—ATMs from lean and obese (high-fat diet–fed) C57Bl/6 mice were analyzed by a combination of flow cytometry, immunofluorescence, and expression analysis for M2a and M1 genes. Pulse labeling of ATMs with PKH26 assessed the recruitment rate of ATMs to spatially distinct regions.

RESULTS—Resident ATMs in lean mice express the M2a marker macrophage galactose N-acetyl-galactosamine specific lectin 1 (MGL1) and localize to interstitial spaces between adipocytes independent of *CCR2* and *CCL2*. With diet-induced obesity, MGL1$^+$ ATMs remain in interstitial spaces, whereas a population of MGL1$^-$CCR2$^+$ ATMs with high M1 and low M2a gene expression is recruited to clusters surrounding necrotic adipocytes. Pulse labeling showed that the rate of recruitment of new macrophages to MGL1$^-$ ATM clusters is significantly faster than that of interstitial MGL1$^+$ ATMs. This recruitment is attenuated in *Ccr2*$^{-/-}$ mice. M2a- and M1-polarized macrophages produced different effects on adipogenesis and adipocyte insulin sensitivity in vitro.

CONCLUSIONS—The shift in the M2a/M1 ATM balance is generated by spatial and temporal differences in the recruitment of distinct ATM subtypes. The obesity-induced switch in ATM activation state is coupled to the localized recruitment of an inflammatory ATM subtype to macrophage clusters from the circulation and not to the conversion of resident M2a macrophages to M1 ATMs in situ. *Diabetes* **57:3239–3246, 2008**

Obesity activates inflammatory pathways in leukocytes that contribute to the pathogenesis of obesity-associated diseases, such as type 2 diabetes and atherosclerosis. In particular, adipose tissue macrophages (ATMs) have been identified as the primary source of inflammatory cytokine production in adipose tissue and a key component in the progression to insulin resistance with obesity. ATMs are increased in visceral fat depots with obesity and correlate with measures of insulin resistance (1). A range of mouse models with loss-of-function mutations in genes important in macrophage recruitment (*Ccr2*), inflammatory cytokine production (*Tnfα*), and proinflammatory activation (*Ikkβ*) have demonstrated protection from high-fat diet–induced insulin resistance (2–4).

Despite these advances, the function of ATMs in lean and obese states is poorly understood. It has been suggested that ATMs influence a range of processes in adipose tissue, including adipogenesis, angiogenesis, and the response to hypoxia (5–7). One potential clue to understanding these diverse functions emerges from the evidence that macrophages can exist in different activation states with distinct properties (8). On stimulation with lipopolysaccharide (LPS) and interferon-γ, macrophages assume a proinflammatory classical activation profile also known as M1. However, under the influence of T$_H$2 cytokines interleukin (IL)-4 or IL-13, macrophages assume an alternative activation state (M2a) and produce immunosuppressive factors, such as IL-10, IL-1RA, and arginase (9). We have previously demonstrated that ATMs in lean mice are polarized toward an alternatively activated state (M2a), whereas ATMs in obese mice have an M1 profile (10). The importance of this M1/M2a balance in glucose metabolism has been illustrated in macrophage-specific *Pparg*$^{-/-}$ mice that have deficient M2a polarization, increased adipose tissue inflammation, and worse insulin resistance (11,12).

How does obesity switch ATMs from an M2a to an M1 activation state? One hypothesis is that resident M2a ATMs are uniformly converted to an M1 state. A second hypothesis is that M1 ATMs are generated by the obesity-induced trafficking of a subset of inflammatory CCR2$^+$ Ly6G^{hi}CX3CR1^{low} monocytes to fat similar to what is seen in atherosclerotic lesions (13). Currently, there is insufficient information to differentiate between these two models. In this study, we provide evidence for the latter model by characterizing subtypes of ATMs in lean and obese mice. We identified a population of resident ATMs expressing the M2a marker macrophage galactose N-acetyl-galactosamine specific lectin 1 (MGL1/CD301) that localizes to interstitial spaces between adipocytes. High-fat diet feeding does not alter the presence of MGL1$^+$ ATMs but instead induces the spatially restricted accumulation of M1-polarized MGL1$^-$ ATMs in clusters surrounding dead adipocytes. Kinetic studies show that the rate of recruitment of these subtypes into adipose tissue differs significantly and support a model in which the M2a-to-M1 switch in ATMs is coupled to differential monocyte/macrophage recruitment.

FIG. 1. Resident M2a ATMs in lean mice are MGL1$^+$ and are recruited independent of CCR2/CCL2. Immunofluorescence localization of ATMs in adipose tissue using confocal microscopy. Samples from male C57Bl/6 mice fed chow diet. Similar results were obtained from three to five independent mice. Bar = 50 μm. *A*: MGL1$^+$ ATMs are present in interstitial spaces between adipocytes in multiple adipose tissue depots. Caveolin staining (red) delineates adipocytes. *B*: MGL1$^+$ cells (red) are macrophages based on costaining with F4/80 (*left panels*) and CD11b (*right panel*). Images from epididymal fat pads. *C*: Perivascular localization of a portion of MGL1$^+$ ATMs. Isolectin (red) labels endothelial cells to highlight vasculature in fat. MGL1$^+$ ATMs express IL-10 (*D*) and CCR2 (*E*). *F*: MGL1$^+$ ATMs are retained in epididymal adipose tissue from *Ccl2$^{-/-}$* and *Ccr2$^{-/-}$* mice. (Please see http://dx.doi.org/10.2337/db08-0872 for a high-quality digital representation of this figure.)

RESEARCH DESIGN AND METHODS

Animal care and use. Male C57Bl/6 mice or *Ccr2$^{-/-}$* mice were fed a normal chow (LabDiet 5001) or high-fat diet (45% kcal from fat, Research Diets) ad libitum for 16–20 weeks from 8 weeks of age. *Ccl2$^{-/-}$* mice were provided by D. Eitzmann (University of Michigan). Animals were housed in a specific pathogen–free facility and given free access to food and water. All animal use was in compliance with the Institute of Laboratory Animal Research Guide for the Care and Use of Laboratory Animals and approved by the University Committee on Use and Care of Animals at the University of Michigan.
Confocal microscopy. Mice were euthanized and slowly perfused by intracardiac injection with 10 ml of 1% paraformaldehyde diluted in PBS. Small fat pad samples were excised and blocked for 1 h in 5% BSA in PBS with gentle rocking at room temperature. For detection of intracellular antigens, blocking and subsequent incubations were done in 5% BSA in PBS with 0.3% Triton X-100. Primary antibodies were diluted in blocking buffer to 0.5–1 μg/ml and added to fat samples for 2 h at room temperature or overnight at 4°C. After three washes, fluorochrome-conjugated secondary antibodies were added for 1 h at room temperature, and nuclei were stained with TOPRO-3. Alexa 647–conjugated isolectin (Molecular Probes) was used to identify vascular structures. Fat pads were imaged on an inverted confocal microscope (Olympus Fluoview 300) by placing the pad in 95% glycerol in a chambered coverslip. Anti-mouse antibodies used were against TLR4 and CCR2 (Santa Cruz Biotechnology); CD11c, CD11b, and Caveolin1 (BD Biosciences); and F4/80 and MGL1 (clone ER-MP23; Abcam).
Macrophage labeling with PKH26. PKH26 (Sigma) was prepared for phagocytic labeling per the manufacturer's instructions. One milliliter of 1 μmol/l PKH26 was injected intraperitoneally into mice fed high-fat diet for 12

weeks. Clusters were imaged by taking 5- to 10-μm *z*-sections, and TOPRO3$^+$F4/80$^+$ cells were scored for PKH26 intracellular staining.
**Flow cytometry and gene expression analysis.** Flow cytometry on stromal vascular fraction (SVF) cells and real-time RT-PCR analysis were performed as previously described (10). Anti-mouse antibodies used were F4/80-PE-Cy5 (eBioscience) and CD301/MGL1 (ABDSerotec).
Macrophage conditioned media and adipocytes. Differentiation, 2-deoxy-glucose uptake assays, and immunoblots of 3T3-L1 adipocytes were performed as described previously (14). Bone marrow macrophages were derived by culturing bone marrow suspensions in Dulbecco's modified Eagle's medium with 10% heat-inactivated fetal bovine serum in the presence of 20% L929 conditioned medium for 7 days.

RESULTS

Resident ATMs reside between adipocytes and express the M2a marker MGL1. We first examined the properties of resident ATMs in lean mice. Consistent with previous studies (10), we observed that ATMs in multiple fat depots uniformly express MGL1, an established marker of alternative M2a macrophage activation (Fig. 1*A*) (15,16). MGL1$^+$ ATMs were uniformly F4/80$^+$ and CD11b$^+$ and resided in interstitial spaces between adipocytes in lean mice (Fig. 1*B*). These ATMs were occasionally associated with blood vessels but were not restricted to
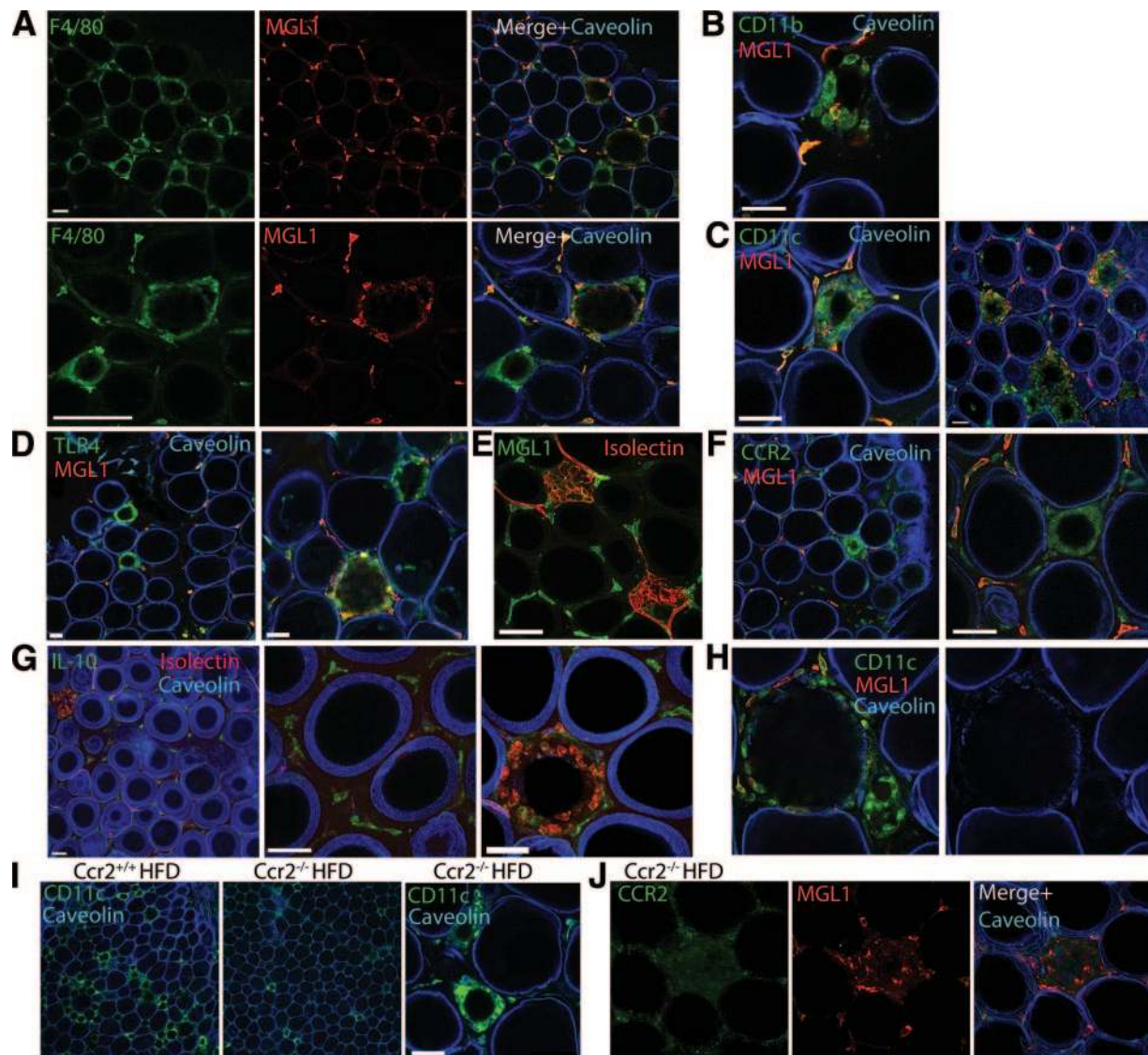
FIG. 2. ATMs in clusters in obese mice are MGL1⁻CCR2⁺ and MGL1⁺ ATMs are retained. Characterization of ATMs in high-fat diet (HFD)-fed C57Bl/6 mice. Caveolin staining (blue) demonstrates loss of membrane integrity in lipid droplets. Staining patterns were observed in at least four independent mice. Bar = 50 μm. A and B: Interstitial ATMs are retained with obesity and are uniformly MGL1⁺F4/80⁺CD11b⁺. CD11c (C) and TLR4 (D) are strongly expressed in MGL1⁻ ATMs in clusters. Isolectin binding (E) and CCR2 expression (F) are increased in ATM clusters and do not overlap with MGL1 expression. G: IL-10 expression is retained in interstitial ATMs and is downregulated in ATM clusters. H: Partial loss of caveolin staining in a dying adipocyte surrounded by a thin wall of MGL1⁻CD11c⁺ ATMs. I: Reduced numbers of ATM clusters in epididymal fat in high-fat diet Ccr2⁻/⁻ mice. ATM clusters in Ccr2⁻/⁻ mice express CD11c similar to obese Ccr2⁺/⁺ mice. J: ATM clusters in Ccr2⁻/⁻ mice downregulate MGL1 expression. (Please see http://dx.doi.org/10.2337/db08-0872 for a high-quality digital representation of this figure.)

perivascular regions (Fig. 1*C*). Reinforcing their M2a polarization, MGL1⁺ resident ATMs also express IL-10 (Fig. 1*D*).

To understand the mechanism of recruitment of MGL1⁺ ATMs, we examined the expression of chemokine receptors previously implicated in macrophage migration. MGL1⁺ ATMs expressed CCR2 (Fig. 1*E*); however, the localization and quantity of the MGL1⁺ ATMs were not altered in visceral fat pads from $Ccr2^{-/-}$ and $Ccl2^{-/-}$ mice (Fig. 1*F*). This demonstrates that MGL1⁺ ATMs are recruited to fat via CCR2- and CCL2-independent mechanisms.

Obesity induces the accumulation of MGL1⁻ ATMs in adipose tissue while retaining MGL1⁺ interstitial ATMs. The M2a marker MGL1 permitted the examination of how obesity biases ATMs toward an M1 activation state. If obesity alters the phenotype of all resident ATMs, we predicted that MGL1 expression might be decreased in all ATMs with high-fat diet. However, we observed that MGL1

expression was retained in interstitial ATMs in high-fat diet–fed mice, despite adipocyte hypertrophy and ongoing adipocyte death (Fig. 2*A*). In contrast, ATMs in clusters ("crown-like structures") were uniformly MGL1⁻. Occasional MGL1⁺ ATMs were observed toward the outer rim of the clusters. To see if this heterogeneity of MGL1 expression is found in other models of obesity, ATMs in *db/db* mice were examined and found to have an identical distribution of MGL1⁺ ATMs in interstitial spaces and MGL1⁻ ATMs confined to clusters (supplementary Fig. 1, available in an online appendix at http://dx.doi.org/10.2337/db08-0872).

The MGL1⁻ ATMs in clusters were F4/80⁺ and CD11b⁺ and expressed high levels of inflammatory markers CD11c and TLR4, although these were also expressed to some degree in MGL1⁺ ATMs (Fig. 2*B–D*). In contrast, MGL1⁻ ATMs had high affinity for isolectin, a previously identified marker for inflammatory ATMs (5), whereas MGL1⁺ ATMs

did not bind isolectin (Fig. 2*E*). MGL1$^-$ ATMs in clusters also had high CCR2 expression, whereas the interstitial MGL1$^+$ ATMs had low CCR2 expression (Fig. 2*F*). Conversely, IL-10 expression was prominent in interstitial ATMs and downregulated in the ATM clusters (Fig. 2*G*). Overall, these results suggest that M1 activation of ATMs is spatially restricted to ATM clusters and is superimposed on the MGL1$^+$ ATM population seen in lean mice.

ATM clusters were closely associated with vascular structures (Fig. 2*E*) and surrounded lipid droplets from dead adipocytes that were caveolin negative. Some adipocytes were identified with a discontinuous distribution of caveolin at the membrane and were surrounded by a thin layer of macrophages, suggesting that this is an early lesion (Fig. 2*H*). Uniformly, lipid droplets surrounded by multiple layers of macrophages were caveolin negative, consistent with coordinated regulation of M1 ATM clustering and adipocyte death. This suggests that loss of adipocyte membrane integrity is the likely initiating event for MGL1$^-$ ATM accumulation.

To assess the importance of CCR2 for MGL1$^-$ ATM accumulation, obese *Ccr2*$^{-/-}$ mice were analyzed. Compared with *Ccr2*$^{+/+}$ mice, *Ccr2*$^{-/-}$ mice had fewer ATM clusters (Fig. 2*I*). However, the ATMs in these clusters were similar to those seen in *Ccr2*$^{+/+}$ mice in that they were CD11c$^+$ and MGL1$^-$ (Fig. 2*J*). In these mice, all F4/80$^+$ ATMs were also CD11c$^+$ (supplementary Fig. 2, available in the online appendix). This suggests that CCR2-independent mechanisms exist to recruit MGL1$^-$ ATMs to clusters.

Diet-induced obesity induces the recruitment of M1-polarized MGL1$^-$ ATMs into visceral fat. The imaging data suggested that the primary difference between ATMs in lean and obese mice is the accumulation of MGL1$^-$ ATMs. To confirm this, we analyzed the SVF from adipose tissue from lean and obese mice by flow cytometry. Of ATMs in both epididymal and subcutaneous fat pads from lean mice, >80% were MGL1$^+$ (Fig. 3*A*). In high-fat diet–fed mice, there was a decrease in the percentage of MGL1$^+$ ATMs in epididymal fat (Fig. 3*B*). This decrease was accompanied by a 2.5-fold increase in the percentage of MGL1$^-$ ATMs in obese mice with high-fat diet. These changes resulted in a shift in the ratio of M2a to M1 ATMs from 4:1 in normal diet–fed mice to 1.2:1 in high-fat diet–fed mice. We next examined ATMs from subcutaneous fat and found that the percentage of MGL1$^+$ ATMs was not changed with high-fat diet in this fat depot. Like visceral fat, high-fat diet induced the accumulation of MGL1$^-$ ATMs in subcutaneous fat, but the accumulation of MGL1$^-$ ATMs in subcutaneous fat was less than what was observed for visceral fat.

To verify that MGL1$^+$ and MGL1$^-$ ATMs have different activation profiles, gene expression was analyzed in the two ATM populations isolated from obese mice. Compared with MGL1$^-$ ATMs, MGL1$^+$ ATMs had increased expression of M2a macrophage genes *Il10*, *Arg1*, and *Pgc1b* (Fig. 3*C*). In contrast, MGL1$^-$ ATMs had significantly higher expression of inflammatory genes *Nos2* and *Il1b*, consistent with a proinflammatory activation state. Examination of other proinflammatory genes demonstrated trends of higher expression of *Ccl3* and *Ccl4* in MGL1$^-$ ATMs relative to MGL1$^+$ ATMs.

MGL1$^-$ ATMs are recruited to clusters at a faster rate than MGL1$^+$ interstitial ATMs. The spatial separation between MGL1$^-$ and MGL1$^+$ ATMs in obesity suggests that these subtypes are recruited to adipose

tissue via different mechanisms. To evaluate this, we used PKH26 labeling to identify newly recruited ATMs. Mice were injected with PKH26 that label ATMs with near 100% efficiency (17). Because this inert dye is taken up by macrophages and not monocytes (18), ATMs recruited to adipose tissue after the time of injection can be identified as F4/80$^+$PKH26$^-$ cells. Because this experiment is dependent on similar rates of retention of the PKH26 dye in M1- and M2-polarized macrophages, we examined PKH26 dye staining in macrophages stimulated with vehicle, LPS, or IL-4 (supplementary Fig. 3, available in the online appendix). This demonstrated that the intracellular retention of PKH26 dye was not altered by macrophage activation with LPS or IL-4 for up to 7 days.

After 12 weeks of high-fat diet feeding, mice were injected with PKH26 and were analyzed at different times after injection for F4/80$^+$PKH26$^-$ ATMs. Three days after injection, almost all ATMs in both clusters and interstitial spaces were PKH26$^+$ (Fig. 4*A*). With increasing time after injection, the percentage of PKH26$^-$ ATMs in the clusters steadily increased, which suggests that new ATMs were recruited specifically to the clusters (Fig. 4*B*). In contrast, the proportion of PKH26$^-$ ATMs in interstitial spaces remained low throughout the time course, suggesting that ATMs traffic to interstitial areas at a significantly slower rate than they traffic to clusters.

These results suggested that MGL1 expression defines the differentially recruited ATM subtypes identified by PKH26 labeling. By confocal microscopy, the majority of the PKH26$^-$ ATMs in clusters were MGL1$^-$, and interstitial cells with retained PKH26 label were MGL1$^+$ (Fig. 4*C*). To confirm this, ATMs were analyzed by flow cytometry 28 days after PKH26 injection (Fig. 4*D*). This showed that PKH26$^+$F4/80$^+$ ATMs were MGL1$^+$, whereas PKH26$^-$F4/80$^+$ had low MGL1 expression.

To assess how CCR2 deficiency alters these recruitment dynamics, we injected high-fat diet–fed *Ccr2*$^{-/-}$ mice with PKH26 and analyzed the appearance rate of ATMs in clusters and in interstitial spaces. The percentage of PKH26$^-$F4/80$^+$ cells in clusters 28 days after injection from *Ccr2*$^{-/-}$ mice was decreased compared with *Ccr2*$^{+/+}$ mice, which suggests that ATMs are recruited to clusters at a slower rate in the absence of CCR2 (Fig. 4*E*). The accumulation of new interstitial ATMs was not altered in *Ccr2*$^{-/-}$ mice, consistent with our previous results (Fig. 1*F*).

M1- and M2a-activated macrophages have different effects on adipogenesis and glucose uptake. The differences between ATM subsets suggest that M1 and M2a macrophages may have different effects on adipocyte function. To test this, we used conditioned media from untreated, LPS-stimulated (M1), and IL-4–stimulated (M2a) macrophages in assays with 3T3-L1 adipocytes. These activation conditions generated the expected macrophage phenotypes: LPS stimulated tumor necrosis factor-α and IL-12 production, whereas IL-4 induced arginase and MGL1 (data not shown). Insulin-stimulated glucose uptake was inhibited by M1 conditioned medium but not with conditioned media from M2a or unstimulated macrophages (Fig. 5*A*). Additionally, when preadipocytes were differentiated in the presence of conditioned media conditions, we observed similarly that whereas M1 conditioned medium effectively inhibited adipogenesis, conditioned media from control and M2a macrophages were permissive to adipogenesis even when added at high concentrations (Fig. 5*B* and *C*).
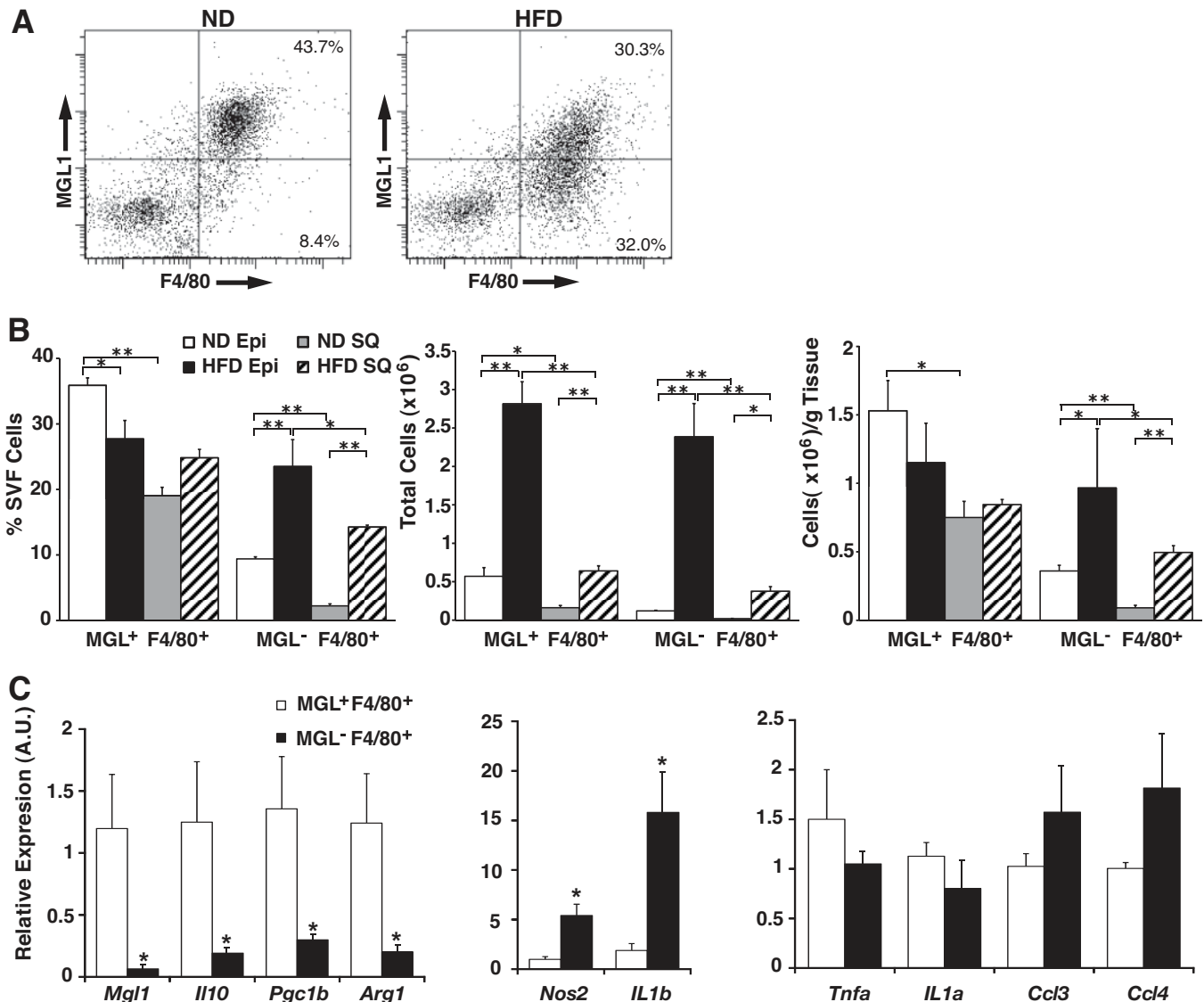
FIG. 3. Obesity induces the recruitment of M1 MGL1$^-$ ATMs to adipose tissue. *A*: Accumulation of MGL1$^-$ ATMs with high-fat diet (HFD) feeding. SVF was isolated from epididymal fat pads and stained to identify MGL1$^+$ and MGL1$^-$ F4/80$^+$ ATMs. Percentages of total SVF provided from a representative experiment. Similar results were observed for six animals per group. *B*: Induction of MGL1$^-$F4/80$^+$ ATMs with obesity is more pronounced in visceral compared with subcutaneous fat. ATM MGL1 subtypes were quantitated by flow cytometry and expressed as a percentage of SVF, total cells per fat pad, and total cells per gram fat. Visceral fat from epididymal fat pads (Epi) were compared with subcutaneous fat (SQ) from the inguinal fat pad. *n* = 6 per group. Values are expressed as means ± SE. *P < 0.05. **P < 0.005. *C*: Differential inflammatory gene expression between ATM subtypes shows M2a polarization of MGL1$^+$ ATMs. MGL1$^+$ and MGL1$^-$ ATMs were isolated by fluorescence-activated cell sorting, and RNAs were prepared for real-time RT-PCR analysis. Gene expression is expressed as relative to MGL1$^+$ ATMs. M2a genes (*left panel*) and M1 genes (*right panels*) were analyzed. *n* = 4 per group. Values are expressed as means ± SE. *P < 0.05. A.U., arbitrary units; ND, normal diet.

DISCUSSION

Our studies address several gaps in what is known about ATMs. Our data demonstrate that ATMs in lean mice extensively localize to interstitial spaces between adipocytes and reinforce the concept that ATMs are a fundamental component of adipose tissue even in lean states. These "resident ATMs" uniformly express markers of M2a alternative activation, MGL1 and IL-10. MGL1 is strongly induced by IL-4/IL-13 in macrophages in vitro but is expressed in dermal macrophages independent of IL-4 or IL-13, suggesting that multiple inputs regulate MGL1 expression (15). MGL1 is expressed in a subtype of macrophages involved in granuloma formation, and *Mgl*1$^{-/-}$ mice demonstrate defective tissue repair after injury, consistent with the proposed role for M2a macrophages in tissue remodeling (19).

MGL1$^+$ ATMs are poised to communicate directly with adipocytes, and our in vitro experiments suggest that macrophage activation state is an important variable in this communication. The permissive nature of M2a-polarized conditioned medium on glucose uptake and adipogenesis is consistent with the notion that in lean settings, MGL1$^+$ ATMs promote an environment favorable for new fat cell formation. The inhibition of these processes by M1 macrophages may instead ultimately promote adipocyte hypertrophy and death, which has been closely linked to ATM accumulation (20).

Obesity does not significantly alter the localization of MGL1$^+$ ATMs in adipose tissue but instead superimposes a new population of M1-polarized MGL1$^-$CCR2$^+$ ATMs on these resident cells. A decrease in the quantity of M2a ATMs combined with the appearance of these "recruited
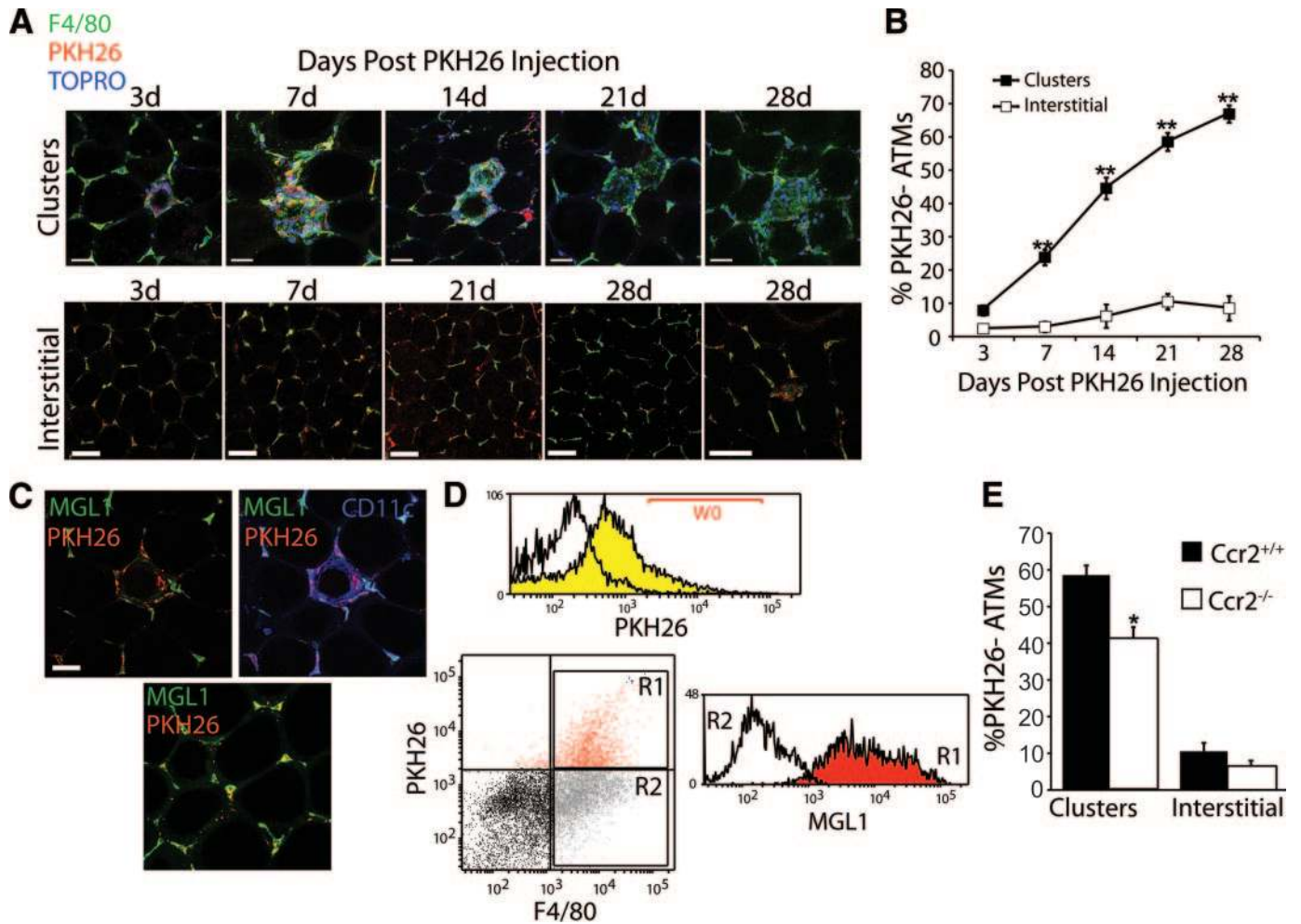
FIG. 4. MGL1⁻ ATMs are preferentially recruited to clusters with high-fat diet feeding. *A* **and** *B*: **Pulse labeling of ATMs demonstrates recruitment of ATMs to clusters and not interstitial sites with high-fat diet feeding.** *A*: **High-fat diet–fed C57Bl/6 mice were injected with PKH26 to label ATMs in visceral fat and analyzed by confocal microscopy at the indicated time after injection. Imaging focused either on ATM clusters (**top**) or interstitial areas (**bottom**). PKH26⁻ ATMs accumulate in clusters while the interstitial ATMs retain PKH26⁺ as long as 28 days after labeling.** *B*: **Quantitation of PKH26⁻F4/80⁺ ATMs during time course. From two to three mice per time point, 25–30 clusters or high-power fields were analyzed and scored for the percentage of PKH26⁻ ATMs. ***P < 0.005 vs. interstitial.** *C* **and** *D*: **MGL1⁺ ATMs preferentially retain PKH26.** *C*: **Immunofluorescence on mice 28 days after PKH26 injection, demonstrating the retention of dye in MGL1⁺ ATMs. PKH26⁻ ATMs are primarily MGL1⁻CD11c⁺ cells in clusters.** *D*: **Flow cytometry of SVF from mice 28 days after PKH26 injection. PKH26⁺ gates (W0) were defined by comparing ATMs from uninjected (white) versus PKH26 injected (yellow) mice 3 days after injection. PKH26⁺ (R1) and PKH26⁻ (R2) ATMs (F4/80⁺) were gated and examined for MGL1 expression. PKH26⁺ ATMs have high MGL1 expression compared with low MGL1 expression in PKH26⁻ ATMs. Representative experiment is shown from one of three independent experiments.** *E*: **Decreased rate of recruitment of ATMs to clusters in obese** *Ccr2⁻/⁻* **mice.** *Ccr2⁻/⁻* **mice were analyzed 28 days after injection by microscopy and scored for the percentage of PKH26⁻ ATMs in clusters or interstitial areas. ***P < 0.05 vs.** *Ccr2⁺/⁺* **mice. (Please see http://dx.doi.org/10.2337/db08-0872 for a high-quality digital representation of this figure.)**

ATMs" ultimately shifts the balance of M1/M2a ATMs to create a more proinflammatory environment in adipose tissue. PKH26 labeling shows that this recruitment is highly spatially restricted to clusters and is consistent with intravital microscopy data that show increased leukocyte trafficking into adipose tissue with obesity (21). We note that it has been reported that isolectin does not label inflammatory clusters of macrophage in the crown-like structures (22). In our experiments, we did not identify heterogeneity in isolectin binding to the clusters because nearly 100% of all clusters are isolectin positive. This may be due to technical differences in the staining approach or differences in the models used (*db/db* in ref. 22 and diet-induced obesity in our study).

Although it has been suggested that macrophages can be converted between M1 and M2a states (23), our results do not support this notion for ATMs. The restricted distribu-

tion of M1 and M2a ATM subtypes instead support a model where obesity induces the specific migration of inflammatory CCR2⁺Ly6GʰⁱCX3CR1ˡᵒʷ monocytes from the circulation to ATM clusters. This is similar to what has been proposed to mediate monocyte/macrophage recruitment to atherosclerotic plaques (24,25). Another hypothesis that we considered was that resident MGL1⁺ ATMs migrate from their interstitial position to the clusters and are subsequently converted to an M1 state. Pulse-labeling ATMs with PKH26 did not support this. If resident ATMs migrate from their interstitial position toward clusters over time, we would expect to observe an increase in PKH26⁺ ATMs in the clusters after labeling and a gradual replacement of interstitial ATMs with PKH26⁻ ATMs. This is not what we observed. Although it is possible that PKH26 is metabolized differently in M1 and M2a ATMs, which would confound our results, in vitro experiments
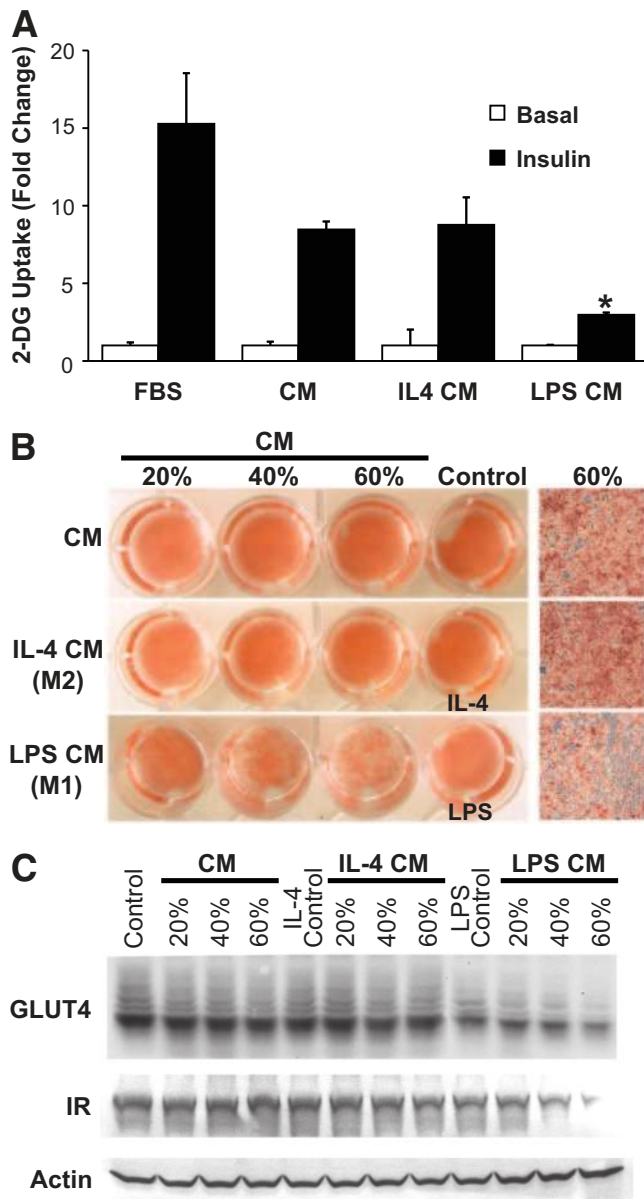
FIG. 5. Differential effects of M1 and M2a macrophages on adipocyte insulin sensitivity and adipogenesis. *A*: Conditioned medium (CM) from M1 but not M2a macrophages blocks insulin-stimulated glucose uptake. Differentiated 3T3-L1 adipocytes were treated with conditioned media from macrophages treated with vehicle, LPS (10 ng/ml), or IL-4 (10 ng/ml) for 12 h and assayed for insulin-stimulated 2-DG uptake, demonstrating selective inhibition with LPS conditioned medium. No effects on glucose uptake were seen with LPS or IL-4 treatment alone. $n = 3$ per group. Values are expressed as means ± SE. *$P < 0.05$. *B*: Conditioned medium from M1 but not M2a macrophages blocks adipogenesis. Conditioned medium from treated macrophages was added during differentiation of 3T3-L1 adipocytes at different percentages by volume, and cells were stained with Oil-Red-O, demonstrating that M2a macrophages are permissive toward adipogenesis in contrast to M1 macrophages. Similar results were from three experiments, and a representative experiment is shown. *C*: Downregulation of GLUT4 and insulin receptor (IR) expression with M1 conditioned medium but not M2a or unstimulated macrophage conditioned medium during adipogenesis. Immunoblots of lysates from 3T3-L1 cells treated with conditioned media during differentiation. (Please see http://dx. doi.org/10.2337/db08-0872 for a high-quality digital representation of this figure.)

did not show that M1 activation per se leads to the loss of the PKH26 dye from macrophages.

Our studies suggest that specifically targeting MGL1⁻ ATMs can potentially decrease high-fat diet–induced in-

flammation in adipose tissue. Blockade of CCR2 has been proposed as one way to accomplish this (2). In this regard, PKH26 labeling showed that $Ccr2^{-/-}$ mice have a decreased rate of accumulation of ATMs in clusters. This is consistent with the evidence that $Ccr2^{-/-}$ mice have few circulating CCR2⁺7/4⁺Ly6G⁻ monocytes because of defective migration out of the bone marrow (13). However, ATM cluster formation is not completely abolished in the absence of CCR2, and these ATMs are still CD11c⁺MGL1⁻F4/80⁺. Therefore, it appears that MGL1⁻ ATMs can be recruited to clusters via CCR2-independent signaling pathways, although CCR2 deficiency may limit this process. This may explain some of the conflicting results published on ATMs in obese $Ccl2^{-/-}$ mice (26,27).

Studies have yet to conclusively support or refute the validity of the M1/M2a model in human ATMs. Consistent with our studies, Bourlier et al. (28) identified ATM subtypes in subcutaneous fat with differential expression of the M2a markers CD206 and CD16 and found that adipose tissue expansion correlated with the accumulation of CD206⁺CD16⁻ ATMs. In contrast, Zeyda et al. (29) failed to identify subsets of ATMs and argued that the ATMs were homogeneous. Both studies failed to identify ATM subtypes with a strict M1 or M2a bias. These studies emphasize that although the identification of M1 and M2a macrophages is fairly mature in mice, it is still unclear how this paradigm applies to human diseases.

Overall, we provide evidence that subtypes of ATMs account for the M2a-to-M1 switch in obesity and can be distinguished by differences in kinetics of accumulation in fat, spatial localization, MGL1 expression, and inflammatory gene expression. This adds to our understanding of ATM biology and provides specific targets for potential intervention. The goal of future studies will be to dissect the molecular signals that govern the migration and recruitment of MGL1⁺ and MGL1⁻ ATMs and to validate this heterogeneity in human adipose tissue.

ACKNOWLEDGMENTS

REFERENCES

1. Harman-Boehm I, Bluher M, Redel H, Sion-Vardy N, Ovadia S, Avinoach E, Shai I, Kloting N, Stumvoll M, Bashan N, Rudich A: Macrophage infiltration into omental versus subcutaneous fat across different populations: effect of regional adiposity and the comorbidities of obesity. *J Clin Endocrinol Metab* 92:2240–2247, 2007

2. Weisberg SP, Hunter D, Huber R, Lemieux J, Slaymaker S, Vaddi K, Charo I, Leibel RL, Ferrante AW: CCR2 modulates inflammatory and metabolic effects of high-fat feeding. *J Clin Invest* 116:115–124, 2005

3. Arkan MC, Hevener AL, Greten FR, Maeda S, Li ZW, Long JM, Wynshaw-Boris A, Poli G, Olefsky J, Karin M: IKK-beta links inflammation to obesity-induced insulin resistance. *Nat Med* 11:191–198, 2005

4. Uysal KT, Wiesbrock SM, Marino MW, Hotamisligil GS: Protection from obesity-induced insulin resistance in mice lacking TNF-alpha function. *Nature* 389:610–614, 1997

5. Cho CH, Koh YJ, Han J, Sung HK, Jong Lee H, Morisada T, Schwendener RA, Brekken RA, Kang G, Oike Y, Choi TS, Suda T, Yoo OJ, Koh GY: Angiogenic role of LYVE-1-positive macrophages in adipose tissue. *Circ Res* 100:e47–e57, 2007

6. Ye J, Gao Z, Yin J, He Q: Hypoxia is a potential risk factor for chronic inflammation and adiponectin reduction in adipose tissue of ob/ob and

dietary obese mice. *Am J Physiol Endocrinol Metab* 293:E1118–E1128, 2007

7. Cinti S, Mitchell G, Barbatelli G, Murano I, Ceresi E, Faloia E, Wang S, Fortier M, Greenberg AS, Obin MS: Adipocyte death defines macrophage localization and function in adipose tissue of obese mice and humans. *J Lipid Res* 46:2347–2355, 2005

8. Mantovani A, Sica A, Sozzani S, Allavena P, Vecchi A, Locati M: The chemokine system in diverse forms of macrophage activation and polarization. *Trends Immunol* 25:677–686, 2004

9. Martinez FO, Sica A, Mantovani A, Locati M: Macrophage activation and polarization. *Front Biosci* 13:453–461, 2008

10. Lumeng CN, Bodzin JL, Saltiel AR: Obesity induces a phenotypic switch in adipose tissue macrophage polarization. *J Clin Invest* 117:175–184, 2007

11. Odegaard JI, Ricardo-Gonzalez RR, Goforth MH, Morel CR, Subramanian V, Mukundan L, Eagle AR, Vats D, Brombacher F, Ferrante AW, Chawla A: Macrophage-specific PPARgamma controls alternative activation and improves insulin resistance. *Nature* 447:1116–1120, 2007

12. Hevener AL, Olefsky JM, Reichart D, Nguyen MT, Bandyopadyhay G, Leung HY, Watt MJ, Benner C, Febbraio MA, Nguyen AK, Folian B, Subramaniam S, Gonzalez FJ, Glass CK, Ricote M: Macrophage PPAR gamma is required for normal skeletal muscle and hepatic insulin sensitivity and full antidiabetic effects of thiazolidinediones. *J Clin Invest* 117:1658–1669, 2007

13. Tsou CL, Peters W, Si Y, Slaymaker S, Aslanian AM, Weisberg SP, Mack M, Charo IF: Critical roles for CCR2 and MCP-3 in monocyte mobilization from bone marrow and recruitment to inflammatory sites. *J Clin Invest* 117:902–909, 2007

14. Lumeng CN, Deyoung SM, Saltiel AR: Macrophages block insulin action in adipocytes by altering expression of signaling and glucose transport proteins. *Am J Physiol Endocrinol Metab* 292:E166–E174, 2007

15. Dupasquier M, Stoitzner P, Wan H, Cerqueira D, van Oudenaren A, Voerman JS, Denda-Nagai K, Irimura T, Raes G, Romani N, Leenen PJ: The dermal microenvironment induces the expression of the alternative activation marker CD301/mMGL in mononuclear phagocytes, independent of IL-4/IL-13 signaling. *J Leukoc Biol* 80:838–849, 2006

16. Raes G, Brys L, Dahal BK, Brandt J, Grooten J, Brombacher F, Vanham G, Noel W, Bogaert P, Boonefaes T, Kindt A, Van den Bergh R, Leenen PJ, De Baetselier P, Ghassabeh GH: Macrophage galactose-type C-type lectins as novel markers for alternatively activated macrophages elicited by parasitic infections and allergic airway inflammation. *J Leukoc Biol* 77:321–327, 2005

17. Lumeng CN, Bodzin JL, Deyoung SM, Saltiel AR: Increased inflammatory properties of adipose tissue macrophages recruited during diet induced obesity. *Diabetes* 6:16–23, 2007

18. Maus U, Herold S, Muth H, Maus R, Ermert L, Ermert M, Weissmann N, Rosseau S, Seeger W, Grimminger F, Lohmeyer J: Monocytes recruited into the alveolar air space of mice show a monocytic phenotype but upregulate CD14. *Am J Physiol Lung Cell Mol Physiol* 280:L58–L68, 2001

19. Sato K, Imai Y, Higashi N, Kumamoto Y, Onami TM, Hedrick SM, Irimura T: Lack of antigen-specific tissue remodeling in mice deficient in the macrophage galactose-type calcium-type lectin 1/CD301a. *Blood* 106:207–215, 2005

20. Strissel KJ, Stancheva Z, Miyoshi H, Perfield JW 2nd, DeFuria J, Jick Z, Greenberg AS, Obin MS: Adipocyte death, adipose tissue remodeling, and obesity complications. *Diabetes* 56:2910–2918, 2007

21. Nishimura S, Manabe I, Nagasaki M, Seo K, Yamashita H, Hosoya Y, Ohsugi M, Tobe K, Kadowaki T, Nagai R, Sugiura S: In vivo imaging in mice reveals local cell dynamics and inflammation in obese adipose tissue. *J Clin Invest* 118:710–721, 2008

22. Nishimura S, Manabe I, Nagasaki M, Hosoya Y, Yamashita H, Fujita H, Ohsugi M, Tobe K, Kadowaki T, Nagai R, Sugiura S: Adipogenesis in obesity requires close interplay between differentiating adipocytes, stromal cells, and blood vessels. *Diabetes* 56:1517–1526, 2007

23. Stout RD, Jiang C, Matta B, Tietzel I, Watkins SK, Suttles J: Macrophages sequentially change their functional phenotype in response to changes in microenvironmental influences. *J Immunol* 175:342–349, 2005

24. Swirski FK, Libby P, Aikawa E, Alcaide P, Luscinskas FW, Weissleder R, Pittet MJ: Ly-6C monocytes dominate hypercholesterolemia-associated monocytosis and give rise to macrophages in atheromata. *J Clin Invest* 117:195–205, 2007

25. Bouhlel MA, Derudas B, Rigamonti E, Dievart R, Brozek J, Haulon S, Zawadzki C, Jude B, Torpier G, Marx N, Staels B, Chinetti-Gbaguidi G: PPARgamma activation primes human monocytes into alternative M2 macrophages with anti-inflammatory properties. *Cell Metab* 6:137–143, 2007

26. Inouye KE, Shi H, Howard JK, Daly CH, Lord GM, Rollins BJ, Flier JS: Absence of CC chemokine ligand 2 does not limit obesity-associated infiltration of macrophages into adipose tissue. *Diabetes* 56:2242–2250, 2007

27. Kanda H, Tateya S, Tamori Y, Kotani K, Hiasa K, Kitazawa R, Kitazawa S, Miyachi H, Maeda S, Egashira K, Kasuga M: MCP-1 contributes to macrophage infiltration into adipose tissue, insulin resistance, and hepatic steatosis in obesity. *J Clin Invest* 116:1494–1505, 2006

28. Bourlier V, Zakaroff-Girard A, Miranville A, De Barros S, Maumus M, Sengenes C, Galitzky J, Lafontan M, Karpe F, Frayn KN, Bouloumie A: Remodeling phenotype of human subcutaneous adipose tissue macrophages. *Circulation* 117:806–815, 2008

29. Zeyda M, Farmer D, Todoric J, Aszmann O, Speiser M, Gyori G, Zlabinger GJ, Stulnig TM: Human adipose tissue macrophages are of an anti-inflammatory phenotype but capable of excessive pro-inflammatory mediator production. *Int J Obes* 31:1420–1428, 2007